curvature of the quasi-spherical C_{60} molecules takes non-nearest-neighbor carbon atoms on adjacent spheres further from each other than the corresponding atoms on adjacent graphite sheets.

Computation of the vacancy formation energy is more straightforward. As long as relaxation can be neglected, then the energy of vacancy formation is just the negative of half the sublimation energy since, by definition, half of all bonds that are broken when a molecule is removed are reconstituted when the molecule is placed on a surface. This gives a vacancy formation energy of 20 kcal/mol, which is comparable to the vacancy formation energy in face-centered cubic metals and much larger than that for rare gases. The reason for this, of course, is the large size of the molecule. Sixty atoms are involved in forming a molecular vacancy.

VII. Summary and Conclusion

The pairwise central force model was applied to certain molecular properties of C_{60}. Starting with a potential whose constants were determined from the energy of sublimation and the lattice parameter of solid C_{60}, it was used to compute the second virial coefficient of the gas phase, the compressibility, the lattice vibrational specific heat, the surface energy, and the vacancy formation energy of the solid. Not many experimental data are available for comparison, but the results are consistent with existing data.

Registry No. C_{60}, 99685-96-8.

(11) Fischer, J. E.; Heiney, P. A.; McGhie, A. R.; Romanow, W. J.; Denenstein, A. M.; McCauley, J. P., Jr.; Smith, Amos B., III. *Science* **1991**, *252*, 1288.

Model for the Dissolution of Calcium Hydroxyapatite Powder

S. Mafé,[†,§] J. A. Manzanares,[†,§] H. Reiss,*[,†] J. M. Thomann,[‡] and P. Gramain[‡]

Department of Chemistry, University of California, Los Angeles, California 90024, and Institut Charles Sadron, CNRS, 67083 Strasbourg Cedex, France *(Received: July 31, 1991; In Final Form: September 11, 1991)*

A physical model for the dissolution of calcium hydroxyapatite (HAP) is proposed. The experimentally observed self-inhibiting dissolution mechanism is modeled by using the scaled particle theory of hard disks. A Langmuir adsorption isotherm is proposed for the formation of a calcium-rich layer on the surface that constitutes a charged interface inhibiting dissolution. The model provides a quantitative explanation of a number of experimental facts. HAP is the main constituent of bone and dental inorganic tissues, and the proposed theory may constitute a new approach for studying related important phenomena like carious processes.

I. Introduction

Calcium hydroxyapatite (HAP) is the main constituent of biological hard tissues such as the bone and dental inorganic tissues, and its chemical behavior forms a model for the study of important biological phenomena such as carious processes. Therefore, the dissolution mechanism of synthetic or natural HAP in acid media has been extensively analyzed (see refs 1-8 and references therein). A series of experimental studies on the kinetics of dissolution of calcium HAP powder[4,7,8] and human enamel powder[5,6] has been presented by Gramain and co-workers. In particular, the systematic analysis of calcium HAP powder dissolution reported in refs 7 and 8 has been conducted very carefully from the experimental viewpoint, but the proposed theoretical model is based on a rather phenomenological approach. This approach gives a simple first-order law having a rate-reduction factor for the flux of the hydrogen ions causing the dissolution of the HAP. The aim of this paper is to provide a *new, simple physical model* for the formation of a calcium-rich layer of low apparent permeability to protons on the HAP surface. The model leads to a self-inhibiting mechanism that explains the observed rate-reduction factor, allowing the layer that forms to protect the surface of HAP from continuous dissolution caused by acid attack. The proposed model is based on a Langmuir isotherm[9] for the calcium ions adsorbed onto the HAP surface, a hard disk theory[10] that automatically provides a decrease in the HAP surface area available for attack by hydrogen ions as calcium adsorption is increased, and a simplified form of the Nernst-Planck equation for the calcium transport through the boundary layer[11] between the HAP surface and the bulk solution.

The structure of the paper is as follows. First, we introduce the dissolution reaction, present the physical model, and carefully discuss the simplifying assumptions. Later, we evaluate the Langmuir adsorption isotherm parameters and compare the model with experiment. Finally, we give some plausibility arguments for the order of magnitude of our results. The study of the dissolution of HAP involves many concepts from physics and chemistry and poses a really multidisciplinary problem. It is hoped that by giving a particular physical picture for the HAP dissolution, future experiments aimed to understand the complex interface behavior can be designed and, ultimately, new ideas for

[†] University of California.
[‡] Institut Charles Sadron.
* To whom correspondence should be addressed.
[§] Permanent address: Department of Thermodynamics, University of Valencia, 46100 Burjasot, Spain.

(1) Fawzi, M. B.; Fox, J. L.; Dedhiya, M. G.; Higuchi, W. I.; Hefferren, J. J. *J. Colloid Interface Sci.* **1978**, *67*, 304.
(2) Fox, J. L.; Dedhiya, M. G.; Higuchi, W. I.; Fawzi, M. B.; Wun, M. *J. Colloid Interface Sci.* **1978**, *67*, 312.
(3) Griffith, E. N.; Katdare, A.; Fox, J. L.; Higuchi, W. I. *J. Colloid Interface Sci.* **1978**, *67*, 331.
(4) Gramain, P.; Voegel, J. C.; Grumpper, M.; Thomann, J. M. *J. Colloid Interface Sci.* **1987**, *118*, 148.
(5) Gramain, P.; Thomann, J. M.; Grumpper, M.; Voegel, J. C. *J. Colloid Interface Sci.* **1989**, *128*, 370.
(6) Thomann, J. M.; Voegel, J. C.; Grumpper, M.; Gramain, P. *J. Colloid Interface Sci.* **1989**, *132*, 403.
(7) Thomann, J. M.; Voegel, J. C.; Gramain, P. *Calcif. Tissue Int.* **1990**, *46*, 121.
(8) Thomann, J. M.; Voegel, J. C.; Gramain, P. *Colloids Surf.* **1991**, *54*, 145.
(9) Adamson, A. W. *Physical Chemistry of Surfaces*; Wiley: New York, 1982.
(10) Reiss, H.; Frisch, H. L.; Lebowitz, J. L. *J. Chem. Phys.* **1959**, *31*, 369. Helfand, E.; Frisch, H. L.; Lebowitz, J. L. *Ibid.* **1961**, *34*, 1037. Reiss, H.; Schaaf, P. *Ibid.* **1989**, *91*, 2514. Speedy, R. J.; Reiss, H. *Mol. Phys.* **1991**, *72*, 1015.
(11) Levich, V. G. *Physicochemical Hydrodynamics*; Prentice-Hall: New York, 1963.

0022-3654/92/2096-861$03.00/0

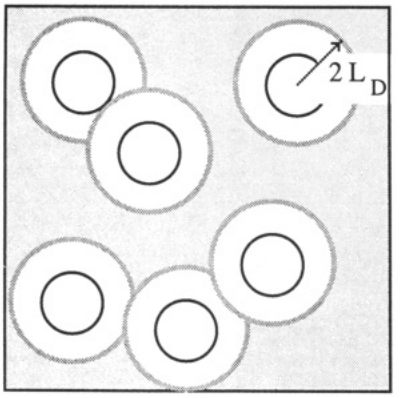

Figure 1. Schematic representation of the adsorbed calcium ions on the HAP surface. Calcium ions are assumed to be hard disks of effective radius $2L_D$.

the study of carious processes will be suggested.

II. Formulation of the Problem

1. Dissolution Reaction of HAP. The dissolution reaction of HAP can be written in the form

$$(n_c - 1)H_2O + Ca_5(PO_4)_3OH \Leftrightarrow 5Ca^{2+} + 3[x_1PO_4^{3-} + x_2HPO_4^{2-} + x_3H_2PO_4^{-} + x_4H_3PO_4] + n_cOH^- \quad (1)$$

where n_c is the number of protons consumed when 1 equiv of HAP is dissolved, and x_i (i = 1–4) define the mole fractions of the different phosphate forms present in the solution. Clearly n_c and the x_i's are related by the demands of stoichiometry. The phosphate ion equilibria are[6]

$$H_3PO_4 \Leftrightarrow H_2PO_4^- + H^+, \quad pK_1 = 2.19 \quad (2.a)$$

$$H_2PO_4^- \Leftrightarrow HPO_4^{2-} + H^+, \quad pK_2 = 7.18 \quad (2.b)$$

$$HPO_4^{2-} \Leftrightarrow PO_4^{3-} + H^+, \quad pK_3 = 12.3 \quad (2.c)$$

If a congruent dissolution is assumed,[8] the hydrogen ion flux J_H and the calcium ion flux J_{Ca} are related through eq 3, where

$$-J_H = R_cJ_{Ca} \quad (3)$$

$R_c = n_c/5$ gives the number of protons consumed when one calcium ion is released. According to eqs 2, we have that

$$R_c = [1 + 3(x_2 + 2x_3 + 3x_4)]/5 \quad (4)$$

It is clear that R_c depends on the pH of the solution through the phosphate equilibria defined by eqs 2. For instance, R_c = 1.43 for pH = 3.5, but R_c = 1.30 for pH = 6.5.

2. Reactive HAP Surface Area: Scaled Particle Theory for Hard Disks and Langmuir Adsorption Isotherm. As stated in the Introduction, the formation of a calcium-rich layer prevents the solid surface of HAP from continuous dissolution by acid attack.[7,8] Here we will simulate this layer by replacing the adsorbed calcium ions and the electrostatically unscreened regions around them by *hard disks*. The equilibrium distribution of disks on the HAP surface is supposed to be the equilibrium distribution of calcium ions that repel each other if they get closer than a screening distance (twice the so-called Debye length, L_D[11]). [In a more sophisticated analysis, the actual variation of the electrostatic potential on the surface, due to an equilibrium distribution of calcium ions would be calculated and the corresponding local flux of hydrogen ions to the surface would be computed as a function of this locally varying potential. In this first approach we use the hard disk model to avoid this obviously difficult theory.] We assume as a first approximation that a hydrogen ion is a disk of the same size as that corresponding to a calcium ion (i.e., both have a radius L_D), even though calcium ions have a higher charge. Figure 1 is a schematic representation of the proposed picture. The dotted disk around each hard disk marks the distance of closest approach between centers and therefore defines the

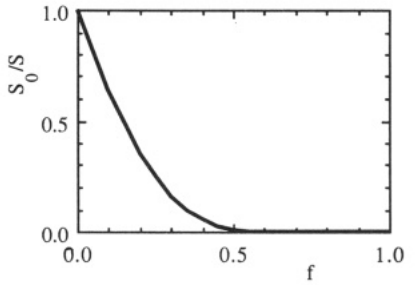

Figure 2. S_0/S vs f according to eq 5 in the text. The plot provides a measurement of the protection afforded by the adsorbed ions as a function of the fraction of surface available for reaction $f = \pi L_D^2N/S$.

"exclusion disk" of an ion, forbidden to the center of another ion. The total surface area of the HAP is denoted by S. The shadowed area outside all the dotted disks represents the domain where hydrogen ions can attack the HAP surface. The relationship between S and the available area for hydrogen attack, S_0, can be very well approximated (at equilibrium) using the scaled particle theory (SPT).[10] It can be shown by means of SPT (see Appendix A) that

$$S_0/S = (1 - f)\exp\{-(3 - 2f)f/(1 - f)^2\}, \quad f \equiv \pi L_D^2N/S \quad (5)$$

where N is the number of disks (adsorbed calcium ions) on the surface. The radius of the disks is taken to be L_D, the electrolyte solution Debye length, which can be estimated as

$$L_D = (\epsilon RT/F^2c_0)^{1/2} \quad (6)$$

In eq 6, ϵ is the dielectric permittivity of the solution (which can be approximated by that of pure water), R is the gas constant, T is the absolute temperature, and F is the Faraday. c_0 is a typical solution concentration, and according to the data in ref 8, it can be represented in our case by c_0 = 0.1 M. Then, $L_D \approx 1.1 \times 10^{-7}$ cm = 11 Å. The total area covered by disks is $\pi L_D^2N = fS$, f being the covered fraction of the surface, i.e., the "packing fraction". Figure 2 is a plot of eq 5 for different values of f. It is clear from this figure that the fraction S_0/S decreases dramatically beyond f = 0.4. This fraction provides an index of the protection afforded by the adsorbed calcium ions.

To employ eq 5 in each practical case, we need to estimate the number N of ions adsorbed on the surface. This can be calculated from the surface concentration of adsorbed calcium c_a as follows:

$$N = N_ASc_a = N_ASn_s\frac{\kappa c_s}{1 + \kappa c_s} \quad (7)$$

where N_A is Avogadro's number. Equation 7 introduces the well-known[9] Langmuir adsorption isotherm for c_a. This adsorption isotherm relates the volume concentration c_s of calcium ions just outside of the adsorption layer with c_a the surface concentration in this layer, through the constants n_s (number of adsorption sites per square centimeter) and κ (a constant exponentially related to the binding energy). The latter are two free parameters to be obtained by fitting theory to experiment. According to eq 7, the fraction of exposed surface is

$$f = \pi L_D^2N_An_s\frac{\kappa c_s}{1 + \kappa c_s} \quad (8)$$

The HAP/solution interface is calcium saturated in the pH range analyzed according to the solubility product of calcium HAP[7,8] in contact with bulk solution. Therefore, c_s in eq 8, as a function of the solution pH, are those characteristic of saturated HAP solutions (see Figure 4 in ref 8).

3. Transport Equation. The transport of calcium ions from the HAP surface to the bulk solution is assumed to occur through a boundary layer of thickness d (see Figure 3). It seems necessary to include this layer in the model since experiments[7,8] show that the dissolution kinetics are stirring-dependent. Figure 3 assumes a quasi-steady state for the calcium transport. This is a reasonable first approximation, since typical experimental times[7,8] are of the

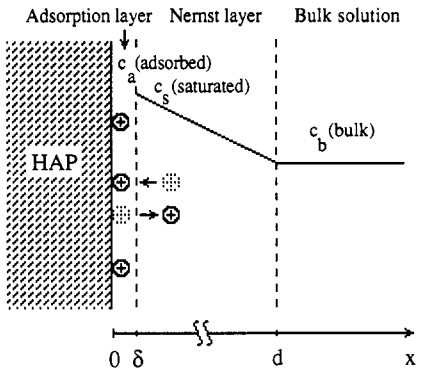

Figure 3. Schematic picture of the concentration profile of calcium ions through a boundary layer of thickness d. We denote by c_a, c_s, and c_b the surface concentration, the volume concentration just outside the adsorption layer, and the bulk concentration of calcium, respectively. A quasi-steady state with a linear concentration profile gradient is assumed.

order of 1 min, while the diffusional relaxation time for calcium ions is $\tau_d = d^2/D_{Ca} \approx 1$ s for $d = 5 \times 10^{-3}$ cm, and a diffusion coefficient $D_{Ca} \approx 10^{-5}$ cm^2/s. Electing to look at the system on this temporal scale means that our treatment ignores (1) the initial time needed for the establishment of an equilibrium layer of adsorbed calcium ions and (2) the transient, i.e., the time evolution of the calcium concentration profile in the boundary layer toward the final linear profile.[12] Moreover, it should also be emphasized that exceedingly long times cannot be allowed in our model if we wish to ignore the change in surface area due to the dissolution of HAP. (A study on the variation of particle size with time under the dissolution conditions of ref 6 can be found in ref 13.) However, according to refs 7 and 8, the surface area corresponding to the "sides" of the HAP platelets is negligible compared to the total area, so that if uniform dissolution is assumed, the change of surface area with time is found to be negligible, at least up to 30% dissolution.[8] We can then analyze the problem without considering changes of the total surface area with time so that the model exhibited in Figure 3 can be used in a wide temporal interval of experimental interest.

The transport equation describing the calcium ion flux is the (simplified) Nernst–Planck equation[11]

$$J_{Ca} = -D_{Ca}\left[\frac{dc}{dx} + 2c\frac{d\phi}{dx}\right] \tag{9}$$

where c is the calcium concentration, x the spatial coordinate, and ϕ the electric potential in units of RT/F. Note that the transport is assumed to occur only in the direction normal to the surface (see Appendices B and C for details). The activity coefficient γ_{Ca} is taken to be constant through the boundary layer. This assumption considerably simplifies the problem and is motivated by the absence of information on the change of γ_{Ca} with concentration for the complex multicomponent system analyzed in refs 7 and 8. Moreover, the use of a supporting electrolyte in the experimental studies (0.08 M potassium chloride in refs 7 and 8) allows us to neglect the term involving the gradient of electric potential in the boundary layer (see ref 11 for a detailed analysis of the validity of this assumption throughout the volume of a boundary layer). In our case, it is clear that the adsorbed calcium ions create an electric field at $x = 0$. However, the concentrated potassium chloride solution employed as supporting electrolyte causes this field to be screened within a few Debye lengths from $x = 0$. Bearing in mind that $d \approx 5 \times 10^{-3}$ cm $\gg L_D \approx 10^{-7}$ cm, it is reasonable to neglect the second term in the right-hand side of eq 9. Thus

$$J_{Ca} \approx -D_{Ca}\frac{dc}{dx} \approx D_{Ca}\frac{c_s - c_b}{d} \tag{10}$$

(12) Dějardin, P. *J. Colloid Interface Sci.* **1989**, *133*, 418.
(13) Hsu, J.; Lin, M. *J. Colloid Interface Sci.* **1991**, *141*, 60. Hsu, J.; Liu, B. *Ibid.* **1991**, *144*, 597.

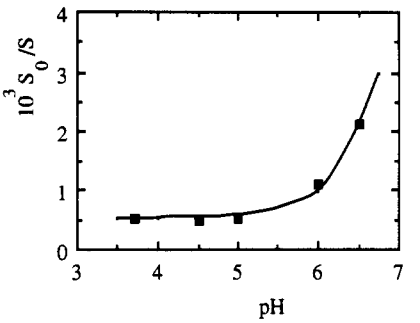

Figure 4. S_0/S vs pH. The full squares represent the experimental points in ref 8. The continuous line corresponds to eq 5 in the text with the adsorption parameters of eq 12.

where the quasi-steady state assumption assumed in Figure 3 has been employed. Note that the effects of stirring observed in refs 7 and 8 can be incorporated into the model through a stirring-dependent value of d. From eqs 3 and 10, it is clear that

$$j_H \equiv J_H S_0 \approx -R_c D_{Ca} S_0 \frac{c_s - c_b}{d} = -\frac{S_0}{S}\left[R_c \frac{D_{Ca} S}{d}(c_s - c_b)\right] \tag{11}$$

where we introduce the total specific surface area S, and refer j_H to mol g^{-1} s^{-1} and J_H to mol cm^{-2} s^{-1}. Equation 11 can be readily compared to the final eq 4 of ref 8. If we define $P^0_{Ca} \equiv D_{Ca}S/d$ and introduce activities a instead of concentrations c, then eq 11 is identical to eq 4 in ref 8, except for the fact that we now have a particular interpretation for the phenomenological coefficient $1/(1 + k)$ introduced in ref 8 to reconcile theory and experiment (this coefficient is (S_0/S) in our model). We will show in the next section that this interpretation of the adherent surface layer can explain the observed dependence[7,8] of $1/(1 + k)$ on experimental conditions.

III. Results

1. Evaluating Parameters κ and n_s of the Adsorption Isotherm. Parameters κ and n_s can be readily evaluated by comparing our theoretical expression for S_0/S (see eqs 5, 8, and 11) to the experimental results for $1/(1 + k)$ in Figure 3 (full line) of ref 8. This latter figure is a plot of $1/(1 + k)$ vs pH obtained from the experimental slopes of the proton uptake fluxes j_H vs mean calcium activities (see Figure 2 of ref 8). The fitting procedure is as follows. First, we choose five different values for the pH and read the corresponding c_s values from the theoretical curve in Figure 4 of ref 8 (calcium concentrations of saturated HAP solutions vs pH). Then, we substitute the values for c_s in eq 8, and the latter into eq 5, so that five different theoretical points $(S_0/S, \text{pH})$ are obtained as functions of the two parameters κ and n_s. On the other hand, from what has been said above the experimental S_0/S values can be read as $1/(1 + k)$ from Figure 3 in ref 9. Finally, a nonlinear least-squares fitting procedure is applied to the set of five points $(S_0/S, \text{pH})$, and the values of the adsorption isotherm parameters are found to be

$$n_s = 2.60 \times 10^{-11} \text{ mol/cm}^2 = 1.56 \times 10^{13} \text{ sites/cm}^2 = 1 \text{ site}/640 \text{ Å}^2 \tag{12.a}$$

$$\kappa = 1.76 \times 10^5 \text{ M}^{-1} \tag{12.b}$$

The experimental value[8] $S = 45$ m^2 g^{-1} has been used in the above computations.

2. Variation of S_0/S with pH. Given the n_s and κ values of eqs 12, it is possible to plot S_0/S vs pH and compare our theory with experiment. This is done in Figure 4, where the experimental points have been read from Figure 3 of ref 8 and are represented by full squares. It seems clear that the agreement between the two parameter theory and experiment is quite good and provides a *physical* interpretation of the phenomenological "rate-reduction factor" $1/(1 + k)$ introduced previously[9] in order to reconcile theory and experiment. [It should be emphasized that such a good agreement cannot be obtained with any other trivial fitting (e.g.,

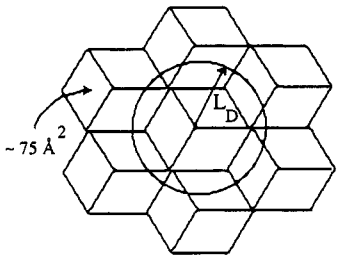

Figure 5. Simplified view of the crystalline HAP surface. A circle of radius $L_D \approx 11$ Å centered at one common vertex is represented.

$S_0/S = A + B \exp(\mathrm{pH})$) or even with three-parameter fittings (e.g., $S_0/S = A + B\,\mathrm{pH} + C\,\mathrm{pH}^2$). Therefore, it is the functional dependence of S_0/S with pH obtained from our physical model which leads to the agreement rather than the fact that we have a two parameter theory.] According to the previous experimental studies,[4,7,8] this reduction factor is caused by the formation of a permselective charged layer on the HAP surface.

Note also that our final equation for j_H has the *same* functional dependence on experimental parameters as eq 4 of ref 9, so that it can also explain a number of experimental facts quoted in that paper. In particular, it is clear that the experimental results in Figure 2 of ref 9 can also be explained from eqs 4, 5, and 11 in our theory. Moreover, the sample conditioning effects, discussed thoroughly in ref 8, can also be understood qualitatively, since in this model the physical state of the interface is specified. However, our model ignores the transient involved in both the formation of the calcium rich layer and the establishment of the diffusional steady state and thus cannot provide a quantitative description of these processes.

IV. Discussion

A model for the dissolution of HAP has been presented. The proposed self-inhibiting mechanisms (Langmuir adsorption plus hard disks approximation) is very simple and introduces only two free parameters, κ and n_s, that characterize the adsorption isotherm. It provides a physical picture by means of which the charged interface, invoked in previous work,[4,7,8] inhibits dissolution. Given the biological importance of calcium HAP, the proposed theory might constitute a first approximation for the study of related important phenomena, e.g., carious processes. Such studies can be motivated by consideration of the orders of magnitude of n_s and S_0/S derived from a comparison of our theory with experiment. To this end, consider the crystallographic data[14] for HAP. The surface of crystalline HAP can be viewed as composed of rhombi of side $a = 9.4$ Å and area $s \approx 75$ Å^2. If we draw a circle of radius L_D centered at one common vertex (see Figure 5), we see that nine rhombi are approximately totally or partially included within it. Suppose now that only one calcium ion can adsorb onto one of these rhombi. Then, we have one adsorption site per 9×75 Å$^2 = 675$ Å^2. This figure can now be compared to the previous result of $n_s = 1$ site/640 Å^2 obtained from our theory. That is, according to our model, if a calcium ion is placed on a site, it protects a minimum area of some 10^3 Å^2 of HAP against dissolution. In fact, this area is much greater because of the exclusion effect introduced in our model via the hard disk theory.

Besides this quantitative agreement, there is the fact that the theory reproduces the experimental requirement that the rate be proportional to $c_s - c_b$. It is not immediately evident that this would have to be the case. For example, if the calcium ions were very mobile, one might expect that the boundary concentration would be sufficiently smeared out, so that it was more like $(S_0/S)c_s$ than c_s itself. Appendices B and C address this point and lead to the conclusion that the adsorbed calcium ions are relatively immobile and that the equilibrium configuration of the disks is established by the constant dissolution of the surface itself.

(14) Lide, D. S., Ed. *CRC Handbook of Chemistry and Physics*; CRC Press: Boca Raton, FL, 1990–1991.

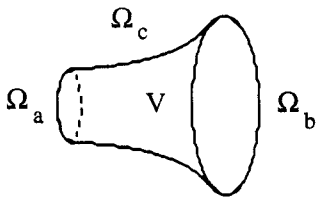

Figure 6. General representation of the volume over which the diverging diffusion of calcium ions occurs. Boundaries Ω_a and Ω_b represent elements of the inner and outer surfaces of the Nernst layer, respectively, while Ω_c is any boundary (impermeable to diffusion) connecting Ω_a and Ω_b.

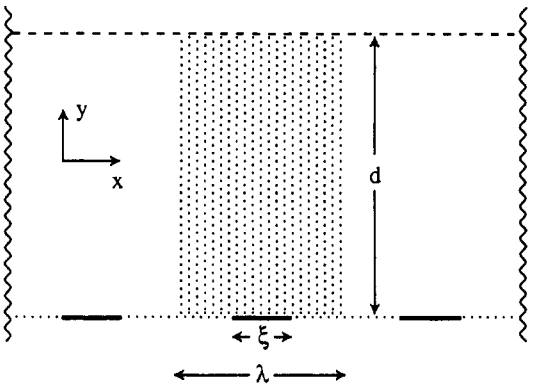

Figure 7. Sketch of the situation considered in Appendix C. The heavy lines at the bottom indicate exposed source lengths.

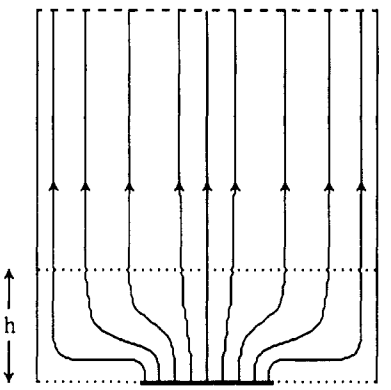

Figure 8. Approximate map of the diffusional flux lines corresponding to the shaded area in Figure 7.

Finally, we must mention that the ideas developed here could be formulated in a more rigorous theoretical basis. In particular, the Langmuir adsorption isotherm is clearly an oversimplified description of the complex kinetics of the problem. For example, to be consistent the isotherm should make use of the available space S_0. Adsorption isotherms incorporating differences in the calcium and hydrogen ions were also attempted, but they did not lead to significant improvement. Therefore, a very simple approach showing some of the experimental trends of the self-inhibiting mechanism was preferred. New experimental data throughout a wider range of pH could motivate the development of a more rigorous theory.

Acknowledgment. Financial support from the Conselleria de Cultura, Educació i Ciencia (Generalitat Valenciana, Spain) and the National Science Foundation, NSF 4-443835-HR-21116, for S.M. and J.A.M. is gratefully acknowledged.

Appendix A. Evaluation of the Reactive Surface Area

The SPT for hard spheres and hard disks can be found elsewhere.[10] We give here a brief exposition of the part of SPT relevant to our theory of HAP dissolution, and derive eq 5 in the text. Suppose a plane of area S contains N particles so that the bulk uniform surface density is $\rho_s = N/S$. Define $P_0(r)$ as the

probability that a circular region of *at least* radius r, free of particle centers, will be found. The empty circular region of radius r is bounded by a circular shell of area $2\pi r\,dr$. Let $\rho(r,\rho_s)$ be the conditional density of centers in this shell. The basic technique is to define a function $G(r,\rho_s)$ so that

$$\rho(r,\rho_s) = \rho_s G(r,\rho_s) \tag{A.1}$$

Thus, $2\pi r\rho_s G(r)\,dr$ has the meaning of the probability of finding a particle center in the shell of a cavity of radius r (we have omitted the explicit dependence of G on ρ_s for the sake of simplicity). The chance that the shell is empty is given by $[1 - 2\pi r\rho_s G(r)\,dr]$, and therefore we have that

$$P_0(r + dr) = P_0(r)[1 - 2\pi r\rho_s G(r)\,dr] \tag{A.2}$$

Upon expansion of the left-hand side of eq A.2 and subsequent integration between $r = 0$ and $r = 1$, using $P(0) = 1$, we obtain

$$P_0(r) = \exp\left\{-\int_0^r 2\pi r\rho_s G(r)\,dr\right\} \tag{A.3}$$

$P_0(r)$ may be given another interpretation. If we denote by $S_0(r)$ the shaded area in Figure 1, then $P_0(r)$ is the fraction $S_0(r)/S$ and represents the probability that a point chosen randomly in the surface S will be located in the shaded region.

Let L_D be the radius of the hard disks. Then the centers of the two particles can never be closer than $2L_D$. It can be shown[10] that function $G(r)$ takes the form

$$G(r) = \begin{cases} \dfrac{1}{1 - \pi r^2\rho_s}, & r < L_D \\ B_0 + \dfrac{B_1}{r}, & r > L_D \end{cases} \tag{A.4}$$

where the first equation in eq A.4 is exact and the second is known to be an excellent approximation.[10] Furthermore the following exact[10] conditions must be satisfied:

$$G(L_{D^-}) = G(L_{D^+}) \qquad G(\infty) = 1 + 2\pi L_D^2\rho_s G(2L_D) \tag{A.5}$$

By applying conditions A.5 to eq A.4, it may be easily shown that

$$B_0 = \frac{1}{(1-f)^2} \qquad B_1 = -L_D\frac{f}{(1-f)^2} \tag{A.6}$$

where f has already been defined in eq 5. Equations A.6 are now substituted into eq A.4 and the resulting function $G(r)$ into the integral in eq A.3, with the result

$$\frac{S_0}{S} \equiv \frac{S_0(r=2L_D)}{S} = P_0(2L_D) = (1-f)\exp\left\{-\frac{(3-2f)f}{(1-f)^2}\right\} \tag{A.7}$$

which is the relation appearing in eq 5.

Appendix B. Dependence of Flux on Boundary Concentrations

It should be noted that in the case under consideration the surface is not homogeneous, so that the diffusive flux of calcium ions diverges from certain surface areas where acid attack takes place. The boundary concentration just out of the reactive domain may be taken equal to c_s, while the concentration in the bulk solution is c_b. However, with a divergent flux, will the total flux still be proportional to $c_s - c_b$?

To examine this question, we look at the general case proposed in Figure 6. The steady-state continuity equation reduces to Laplace's equation

$$\nabla^2 c = 0 \quad \text{over } V \tag{B.1}$$

subject to the boundary conditions

$$c = c_s \quad \text{over } \Omega_a \tag{B.2}$$

$$c = c_b \quad \text{over } \Omega_b \tag{B.3}$$

$$\vec{n}_c\cdot\vec{\nabla}c = 0 \quad \text{over } \Omega_c \tag{B.4}$$

where $\vec{n}_c$ represents the outer unit normal vector of the surface Ω_c (at every point).

The transformation

$$C = \frac{c - c_b}{c_s - c_b} \tag{B.5}$$

changes the above equations to

$$\nabla^2 C = 0 \quad \text{over } V \tag{B.6}$$

$$C = 1 \quad \text{over } \Omega_a \tag{B.7}$$

$$C = 0 \quad \text{over } \Omega_b \tag{B.8}$$

$$\vec{n}_c\cdot\vec{\nabla}C = 0 \quad \text{over } \Omega_c \tag{B.9}$$

Then, Stokes' theorem requires

$$0 = \int\int\int_V \nabla^2 C\,d^3V = \int\int_\Omega \vec{\nabla}C\,d^2\vec{\Omega} = \int\int_{\Omega_a} \vec{\nabla}C\,d^2\vec{\Omega}_a + \int\int_{\Omega_b} \vec{\nabla}C\,d^2\vec{\Omega}_b + \int\int_{\Omega_c} \vec{\nabla}C\,d^2\vec{\Omega}_c \tag{B.10}$$

Note that the last integral in the right-hand side of eq B.10 is equal to zero because of boundary condition B.9. Finally, the total flux can be easily written in the form

$$J = -D\int\int_{\Omega_b} \vec{\nabla}c\,d^2\vec{\Omega}_b = -D(c_s - c_b)\int\int_{\Omega_b} \vec{\nabla}C\,d^2\vec{\Omega}_b = D(c_s - c_b)\int\int_{\Omega_a} \vec{\nabla}D\,d^2\vec{\Omega}_a \tag{B.11}$$

If the surface Ω_b is of relatively infinite extent compared to Ω_a (a configuration that is approximately the case), the Ω_c can be chosen to coincide with some of the outermost flow lines of the diffusion pattern, and eq B.9 will be precisely correct. Furthermore, the bulk of the total flux will have been encompassed since very little will exist beyond these outermost flow lines. Thus it can be seen that eq B.11 is asymptotically exact.

Equation B.11 then implies that in the case of diverging diffusion, the total flux is always proportional to the concentration difference $(c_s - c_b)$, with a proportionality constant dependent on the particular geometry of the system.

Appendix C. Effects Due to the Redistribution of Calcium Ions on the Surface

In Appendix B a divergent flux from a single source was studied. However, the HAP surface contains multiple sources distributed according to the equilibrium configuration of hard disks. Such multiple sources must give rise to a "coupled" flux, and it is necessary to inquire into whether the conclusions of Appendix B can be retained under such coupling. To investigate this question, we examine a two-dimensional situation since the associated flux distribution is easier to diagram in two dimensions. However, the reader will quickly see that no essential change in the results would be occasioned by the treatment of the actual three-dimensional case.

Although the multiple sources are statistically (even if not randomly) distributed, we will compromise the reality of our model by assuming that they are positioned on the sites of a regular lattice. For example, in a two-dimensional case, the picture will resemble Figure 7. Here the heavy lines at the bottom of the figure indicate exposed (reactive) source lengths (areas in the three-dimensional case) while the upper dashed line indicates the limit of the Nernst layer of thickness d. The lattice parameter governing the source locations is λ. The sources themselves are of length ξ so that the spaces between them are of length $\lambda - \xi$. Symmetry allows us to focus on a unit cell of the system like the one shaded in Figure 7.

We introduce an (x,y) coordinate system (y in the vertical direction). The center of the source lies at (0,0) and the boundaries of the unit cell are at $(\pm\lambda/2,0)$. The limit of the Nernst layer lies at $y = d$. The boundary conditions

$$\begin{aligned} \partial c/\partial y = 0 \quad & y = 0 \quad \begin{cases} -\lambda/2 < x < -\xi/2 \\ -\xi/2 < x < \lambda/2 \end{cases} \\ c = c_s \quad & y = 0 \quad -\xi/2 < x < \xi/2 \\ c = c_b \quad & y = d \end{aligned} \tag{C.1}$$

are obvious. The first of eqs C.1 derives from the fact that outside the source and the sink (limit of the Nernst layer) there can be no normal flux. The boundary conditions on the sides of the cell

$$\partial c/\partial x = 0 \qquad x = \pm\lambda/2 \qquad 0 < y < d \tag{C.2}$$

stem from considerations of symmetry (a result of the lattice model). Using eqs C.1 and C.2, it requires very little thought to construct an approximate but essentially correct map of the diffusional flux lines. We exhibit this map in Figure 8.

Because of the boundary conditions, an equivalent of the surface in Figure 6 can be found consisting of the horizontal boundaries represented by the dotted lines at the bottom of the cell together with the vertical boundaries of the cell. Thus, the result of Appendix B applies to this cell and the total flux must be proportional to $c_s - c_b$.

This would complete our argument if it were not for he fact that the reactive areas were determined by the locations of the calcium ions (the disks) that are constantly changing their positions (although maintaining the equilibrium configuration) as the surface dissolves. If this change of configuration is rapid enough the boundary at $y = 0$ would be a "smeared out" uniform entity where the concentration might be something like

$$c(x,0) = (S_0/S)c_s \tag{C.3}$$

Furthermore the flux lines in Figure 8 would be parallel and vertical throughout the length d so that the flux would be

$$J = \frac{D}{d}\left(\frac{S_0}{S}c_s - c_b\right) \tag{C.4}$$

(where D is the diffusion coefficient) and no longer proportional to $c_s - c_b$. We therefore need to estimate the smallest relaxation time of the source distribution that can be tolerated if eq C.4 is not to be in force. This is rather easy to do. Note that in Figure 8 the flux does become uniform, even with an absolutely immobile distribution of sources, above $y = h$. Thus, the flux at $y \geq h$ is essentially ignorant of any reconfiguration of the sources. Also simple scaling ideas indicate that h must have a length of the order of the cell parameter λ. Thus we can set $h = \lambda$ without damaging the validity of our order of magnitude considerations.

Then, in order to avoid having to use eq C.4, it is necessary only for a diffusing particle to traverse the distance $h = \lambda$ in a time less than the relaxation time of the source configuration. Thus, if τ is this relaxation time, we require

$$\lambda^2/D < \tau \tag{C.5}$$

On the real two-dimensional surface there will be N_c exposed reactive areas of average area $\langle s \rangle$ such that $S_0 = N_c\langle s \rangle$. Molecular dynamics studies for disks of diameter $2L_D$ have been performed (last entry of ref 10) to yield both N_c and $\langle s \rangle$ as a function of the packing fraction f. The unit cell in Figure 7 should be assigned (in the three-dimensional case), the area S/N_c and the characteristic length λ is of the order of $(S/N_c)^{1/2}$. At a value of $f = 0.5$, the molecular dynamics result gives

$$\lambda \approx 50L_D \tag{C.6}$$

while D can be estimated as

$$D \approx 10^{-5}\ \text{cm}^2/\text{s} \tag{C.7}$$

Substitution of these numbers into eq C.5 gives $\tau > 7 \times 10^{-6}$ s. Thus, this is the shortest relaxation time that can be tolerated. The longest possible relaxation time τ should be of the order of the rate of dissolution of a single crystalline plane in HAP; it corresponds to a velocity of dissolution of

$$v = a/\tau \tag{C.8}$$

where a is the lattice parameter normal to the direction of dissolution. If we use the estimate $a \approx 10^{-7}$ cm, then eq C.7 gives $v = 10^{-2}$ cm/s. Clearly, the crystal does not dissolve at this enormous velocity, so that $\tau \gg 10^{-5}$ s. As a result, eq C.4 would be inapplicable.

On the other hand, τ might be shorter than the time required for the dissolution of a lattice plane. However, the agreement between theory and experiment, in the sense that the rate is proportional to $c_s - c_b$, suggest that τ is comparable to the time of dissolution of a lattice plane. A simple mechanism for this would involve having the calcium ions so strongly bound to the surface as to be relatively immobile.

Registry No. HAP, 1306-06-5.